Transport Processes and Associated Irreversibilities in Droplet Evaporation

S. K. Dash,* S. P. Sengupta,† and S. K. Som*
Indian Institute of Technology, Kharagpur 721 302, India

To ascertain the process irreversibility in course of evaporation of a liquid drop in a high-temperature convective medium, the instantaneous rate of entropy production and its temporal variation have been determined from the simultaneous numerical solution of the entropy conservation equation, along with the conservation equations of heat, mass, and momentum transports in both the gas and liquid phases. The accuracy of the present numerical experiments has been established from the comparisons of a numerically generated Nusselt number with the relevant empirical and other numerical values available in the literature. From the numerical predictions, a generalized nondimensional correlation is being proposed to express the instantaneous rate of entropy production as a function of pertinent input parameters for droplet evaporation in a convective ambience.

Nomenclature

a = nondimensional radius of droplet, = (a'/a_i')
a' = droplet radius at any instant
a_i' = initial radius of droplet
B = transfer number, = $[Cp^g(T_\infty' - T_s')/\Delta Hv)$
C = mass fraction
C_D = drag coefficient
Cp = specific heat
C_s = mass fraction of liquid vapor at drop surface
$\mathcal{D}$ = diffusivity of vapor in ambience
$\dot{E}'$ = total entropy generation rate
Ec = Eckert number, = $(U_\infty^2/Cp_\infty T_i')$
$\dot{e}'$ = local entropy generation rate per unit volume
Ku = Kutataldze number, = $(\Delta Hv_i/Cp^l T_i')$
k = thermal conductivity
Le = Lewis number
Nu = Nusselt number
P' = pressure
P_a' = normal atmospheric pressure
P_V' = vapor pressure
P_∞' = freestream pressure
Pe = Peclet number, = $(2U_\infty a/\alpha^g)$
Pr = Prandtl number, = $(\mu Cp/k)$
R = characteristic gas constant
$\bar{R}$ = universal gas constant
Re = Reynolds number, = $(2U_\infty a'\rho^g/\mu^g)$
r = nondimensional distance, = (r'/a')
r' = radial coordinate
Sc = Schmidt number, = $(\nu/\mathcal{D})$
T = nondimensional temperature, = (T'/T_i')
T' = temperature
T_i' = initial drop temperature
T_s' = surface temperature
T_∞' = freestream temperature
t = nondimensional time, = $(t'\alpha_i^l/a_i'^2)$
t_d = droplet heat up time
t_l = lifetime of drop
t' = time
U_∞ = freestream velocity
V = nondimensional velocity, = (V'/U_∞)
V' = velocity
V_s' = radial velocity at drop surface
W = molecular weight
Z = transformed coordinate in radial direction
α = thermal diffusivity
γ = ratio of specific heats of freestream gas
ΔHv = latent heat of vaporization of liquid at T_s'
ζ = nondimensional vorticity function, = $(\zeta' a'/U_\infty)$
ζ' = vorticity function
θ = azimuthal coordinate
μ = viscosity
μ_c = chemical potential
ρ = density
ν = kinematic viscosity
ψ = nondimensional stream function, = $[\psi'/(U_\infty a'^2)]$
ψ' = streamfunction

Subscripts
a = of air
i = at the initial stage
r = radial component
v = of vapor
θ = azimuthal component
∞ = of freestream

Superscripts
g = of gas mixture
l = of liquid

Introduction

THE theory of fuel droplet vaporization, due to its inherent impact in various industrial processes, has been under development for several decades and has received a good deal of attention for its theoretical development in recent times. A comprehensive documentation of this work from classical to modern can be found in Marshall,[1] Clift et al.,[2] Law,[3] Faeth,[4] and Sirignano.[5,6] The theory of droplet vaporization plays a key role in understanding the processes of evaporation and combustion of atomized liquid sprays. Though substantial research in the transport processes from drops and sprays has been done recently, the important thermodynamic aspect, namely, the determination of irreversibilities in the process of spray evaporation or combustion, remains almost unexplored. A typical second law analysis of spray evaporation through a basic approach of the estimation of process irreversibilities and the minimization of the same with respect to pertinent input parameters is of prime importance for thermodynamic optimization of the process. As the spray evaporation process is largely associated with a major part of the power industry, the practical implication of second law anal-

Received Dec. 8, 1989; revision received April 26, 1990; accepted for publication May 13, 1990.
*Department of Mechanical Engineering.
†Department of Chemical Engineering.

ysis can be realized through the fact that the total loss in available energy of a power plant is a result of the irreversibilities encountered in the different processes taking place within the system. Similar to the role of transport coefficients of single drops in the conventional modeling of spray evaporation, the information on entropy production rate due to evaporation of an individual drop serves as the fundamental input to the second law analysis of spray evaporation. Quantitative information of the entropy production rate due to the irreversibilities in the entire field of influence of the transport processes in droplet vaporization is hardly found in the literature. The major objective of the present work is geared in this direction. In the first part, the information on the transport processes of an evaporating drop have been generated in a routine manner through the typical solutions of conservation equations for both the phases and has been compared with standard empirical results from literature. In the subsequent part of the work, numerical solution of the entropy conservation equation has been made to establish a functional relationship between the instantaneous entropy generation rate of the process with the controlling input parameters.

Theoretical Formulation

Physical Statement and Assumptions

The physical problem deals with the evaporation of a spherical liquid drop in a convective gaseous medium with a uniform freestream velocity U_∞ with respect to the drop. Freestream temperature T'_∞ is higher than the initial temperature of the drop. The initial Reynolds number Re_i of flow is selected in the range of 10–100. It is assumed that the droplet maintains a perfectly spherical shape at all times because it is very small and its surface tension is high enough so that no distortion at its surface takes place in the range of the Reynolds number studied. It is also assumed that the flowfield is laminar and axisymmetric. Effects due to gravity and thermal radiation are negligible, and thermodynamic equilibrium exists at the gas liquid interface.

The basic objective of the present work is to evaluate the irreversibilities in the process of droplet evaporation that occur due to the effects of heat, mass, and momentum transports in both the gas and droplet phases. This is characterized quantitatively by the rate of entropy production evaluated from the principle of entropy conservation at each and every phase of droplet evaporation. Such a typical irreversibility analysis requires the information on the velocity, temperature, and concentration fields in both the gas and liquid phases at each and every instant. A number of semianalytical and numerical models on droplet evaporation have already been reported in the literature.[7–12] However, it is difficult to incorporate the results from the existing models on the transport processes in droplet evaporation for the evaluation of entropy generation because the temporal variation of velocity, temperature, and concentration fields in droplet and gas phases can not be generated from those results. Hence, the numerical solutions of conservation equations for the transport processes are required to be carried out separately for the present purpose. The pertinent equations and the simplified model in this regard are, therefore, briefly reproduced here for a ready reference.

Transport Processes in Droplet Evaporation

From the comparisons of characteristic time scales for various diffusion and convective transport processes in droplet evaporation, it can be established, following Sundarrajan and Ayyaswamy,[13] that all of the processes, except the energy transport within the drop, can be treated as quasisteady during the lifetime of the drop. Governing equations are written with respect to a spherical polar coordinate system (Fig. 1) with the origin attached to the center of the drop.

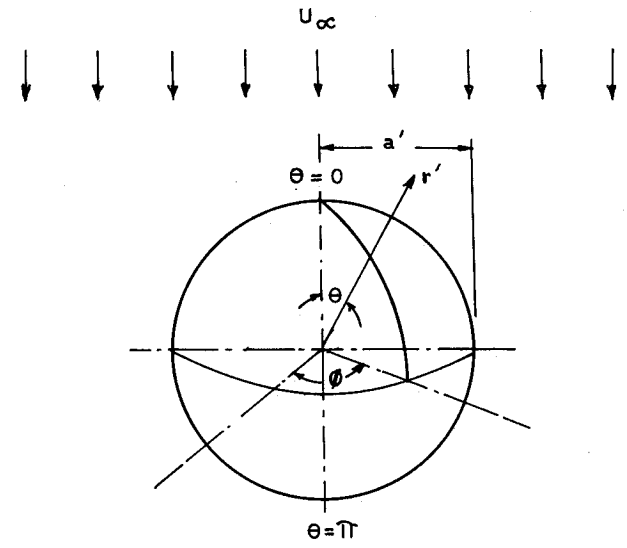

Fig. 1 System of coordinates and nomenclature used in the theoretical analysis.

Momentum

Momentum equations in carrier and liquid phase are written in terms of stream and vorticity functions[14]

Gas phase:

$$\frac{Re}{2}\left[\frac{\partial\psi^g}{\partial r}\frac{\partial}{\partial\theta}\left(\frac{\zeta^g}{r\sin\theta}\right) - \frac{\partial\psi^g}{\partial\theta}\frac{\partial}{\partial r}\left(\frac{\zeta^g}{r\sin\theta}\right)\right]\sin\theta = E^2(E^2\psi^g) \tag{1a}$$

$$E^2\psi^g = \zeta^g r\sin\theta \tag{1b}$$

Liquid phase:

$$\frac{Re}{2}\frac{v^g}{v^l}\left[\frac{\partial\psi^l}{\partial r}\frac{\partial}{\partial\theta}\left(\frac{\zeta^l}{r\sin\theta}\right) - \frac{\partial\psi^l}{\partial\theta}\frac{\partial}{\partial r}\left(\frac{\zeta^l}{r\sin\theta}\right)\right]\sin\theta = E^2(E^2\psi^l) \tag{2a}$$

$$E^2\psi^l = \zeta^l r\sin\theta \tag{2b}$$

where

$$E^2 = \frac{\partial^2}{\partial r^2} + \frac{\sin\theta}{r^2}\frac{\partial}{\partial\theta}\left(\frac{1}{\sin\theta}\frac{\partial}{\partial\theta}\right)$$

Energy

Gas phase:

$$\frac{Pe^g}{2}\left(V_r^g\frac{\partial T^g}{\partial r} + \frac{V_\theta^g}{r}\frac{\partial T^g}{\partial\theta}\right) = \frac{1}{r^2}\frac{\partial}{\partial r}\left(r^2\frac{\partial T^g}{\partial r}\right) + \frac{1}{r^2\sin\theta}\frac{\partial}{\partial\theta}\left(\sin\theta\frac{\partial T^g}{\partial\theta}\right) \tag{3}$$

Liquid phase:

$$\frac{\partial T^l}{\partial t} + \frac{Pe_i^g}{2a}\frac{\alpha_i^g}{\alpha_i^l}\left(V_r^l\frac{\partial T^l}{\partial r} + \frac{V_\theta^l}{r}\frac{\partial T^l}{\partial\theta}\right) = \frac{1}{a^2}\frac{\alpha^l}{\alpha_i^l}\left[\frac{1}{r^2}\frac{\partial}{\partial r}\left(r^2\frac{\partial T^l}{\partial r}\right) + \frac{1}{r^2\sin\theta}\frac{\partial}{\partial\theta}\left(\sin\theta\frac{\partial T^l}{\partial\theta}\right)\right] \tag{4}$$

Species Mass Continuity

Gas phase:

$$\frac{Pe^g}{2}\left(V_r^g\frac{\partial C}{\partial r}+\frac{V_\theta^g}{r}\frac{\partial C}{\partial \theta}\right)$$
$$=\frac{1}{Le^g}\left[\frac{1}{r^2}\frac{\partial}{\partial r}\left(r^2\frac{\partial C}{\partial r}\right)+\frac{1}{r^2\sin\theta}\frac{\partial}{\partial\theta}\left(\sin\theta\frac{\partial C}{\partial\theta}\right)\right] \quad (5)$$

Boundary conditions for the solutions of Eqs. (1–5) are as follows.

At freestream ($r\to\infty$):

$$T^g = T_\infty \quad (6a)$$

$$C = 0 \quad (6b)$$

$$\psi^g = \frac{1}{2}r^2\sin^2\theta + \int_0^\theta V_s\sin\theta\,d\theta \quad (6c)$$

At interface ($r = 1$):

Continuity of tangential velocity

$$\frac{\partial\psi^g}{\partial r} = \frac{\partial\psi^1}{\partial r} \quad (7a)$$

Continuity of tangential stress

$$\frac{\partial}{\partial r}\left(\frac{1}{r^2}\frac{\partial\psi^g}{\partial r}\right) = \frac{\mu^l}{\mu^g}\frac{\partial}{\partial r}\left(\frac{1}{r^2}\frac{\partial\psi^l}{\partial r}\right) \quad (7b)$$

Temperature continuity

$$T^g = T^l \quad (7c)$$

Continuity of heat flux

$$\frac{\partial T^g}{\partial r} = \frac{k^l}{k^g}\frac{\partial T^l}{\partial r}+\frac{1}{2}Pe_i^g Ku\,a\left(\frac{\Delta Hv}{\Delta Hv_i}\frac{Cp_i^g}{Cp^g}\frac{\alpha_i^g}{\alpha^g}\right)V_s \quad (7d)$$

Vapor mass fraction at the drop surface[15]

$$C_s = \frac{1}{1+\left(\frac{W_\infty}{Wv}\right)\left(\frac{P_\infty}{Pv}-1\right)} \quad (7e)$$

At drop center ($r = 0$)

$$\frac{\partial T^1}{\partial r} = 0 \quad (7f)$$

Axisymmetric conditions:

At $\theta = 0$

$$\psi^1 = \psi^g = 0 \quad (8a)$$

$$\zeta^1 = \zeta^g = 0 \quad (8b)$$

$$\frac{\partial T^g}{\partial\theta} = \frac{\partial C}{\partial\theta} = \frac{\partial T^1}{\partial\theta} = 0 \quad (8c)$$

At $\theta = \pi$

$$\psi^g = \int_0^\pi V_s\sin\theta\,d\theta \quad (8d)$$

$$\psi^1 = 0 \quad (8e)$$

$$\zeta^g = \zeta^1 = 0 \quad (8f)$$

$$\frac{\partial T^g}{\partial\theta} = \frac{\partial T^1}{\partial\theta} = \frac{\partial C}{\partial\theta} = 0 \quad (8g)$$

The initial conditions for the solution of Eq. (4) are as follows.

At $t = 0$

$$T^1 = 1 \qquad 0\le r\le 1 \quad (9a)$$

$$T^g = T_\infty \qquad r > 1 \quad (9b)$$

The radial velocity at the droplet surface V_s is found from the consideration of an impermeable interface to the nonevaporating species[15]

$$V_s = \frac{-2(\partial C/\partial r)|r=1}{Re\,Sc(1-C_s)} \quad (10)$$

Depletion of drop diameter with the assumption of its spherical shape is given by

$$\frac{da}{dt} = -\frac{\rho^g}{\rho^l}\frac{Pe_i^l}{2}\bar{V}_s \quad (11a)$$

where $\bar{V}_s$ is the surface averaged value of V_s and is written as

$$\bar{V}_s = \frac{1}{2}\int_0^\pi V_s\sin\theta\,d\theta \quad (11b)$$

Pe_i^l is the initial Peclet number based on thermal diffusivity of liquid as

$$Pe_i^l = 2\,U_\infty\,a_i^l/\alpha_i^l$$

Nusselt Number

Instantaneous values of local and surface averaged Nusselt numbers are found from

$$Nu_\theta = \frac{-2(\partial T^g/\partial r)|r=1}{(T_\infty - T_s)} \quad (12)$$

$$Nu = \frac{1}{2}\int_0^\pi Nu_\theta\sin\theta\,d\theta \quad (13)$$

Irreversibility Analysis

In a continuous field involving heat, mass, and momentum transfer of an incompressible Newtonian fluid in the absence of chemical reaction and body force effects, the local entropy generation rate per unit volume can be written according to Krikwood and Crawford[16] as

$$\dot{e}' = \frac{\mu\Delta:\sigma}{T}+\frac{(-J_q\cdot\nabla T')}{T'^2}+\frac{\Sigma(-J_m\cdot\nabla\mu_c)}{T'}+\frac{\Sigma(-\bar{s}_i J_m\cdot\nabla T')}{T'}$$
$$=\dot{e}_1'+\dot{e}_2'+\dot{e}_3'+\dot{e}_4' \quad (14)$$

where Δ and σ are rate of strain and stress tensors, respectively, J_q and J_m are heat flux and mole flux per unit surface area, respectively, and $\bar{s}_i$ is the partial molal entropy of the species i. The first term in Eqs. (14) is due to fluid friction and can be written for an incompressible Newtonian fluid in spherical polar coordinate system with ϕ symmetry as[17]

$$\dot{e}_1' = \frac{\mu}{T'}\left\{2\left(\frac{\partial V_r'}{\partial r'}\right)^2+2\left(\frac{1}{r'}\frac{\partial V_\theta'}{\partial\theta}+\frac{V_\theta'}{r'}\right)^2+2\left(\frac{V_r'}{r}+\frac{V_\theta'\cot\theta}{r'}\right)^2+\left[r'\frac{\partial}{\partial r'}\left(\frac{V_\theta'}{r'}\right)+\frac{1}{r'}\frac{\partial V_r'}{\partial\theta}\right]^2\right\} \quad (15)$$

The second term in Eqs. (14) is due to heat conduction, the third term pertains to mass transfer, and the fourth term arises from the coupling between heat and mass transfer.

Effects of mass transfer exist only in the carrier phase, which is considered to be a binary mixture of ideal gases (liquid vapor and freestream gas). Chemical potential of liquid vapor in the carrier phase can be written according to Denbigh[18] as

$$\mu c(T', P') = \mu_c^o(T') + \bar{R}T' \ln(P_v'/P') \tag{16}$$

where P' is the total pressure of the ambience and P_v' and $\mu_c^o(T')$ are the partial pressure and the standard state chemical potential of the vapor, respectively. Hence, one can write from Eq. (16)

$$\nabla\mu_c = \frac{\bar{R}T'}{P_v'}\nabla P_v' = \frac{\bar{R}T'}{C} \tag{17}$$

With the help of Eq. (17), the third term of Eqs. (14) can be written as

$$\dot{e}_3' = \frac{\mathcal{D}^g \rho^g \bar{R}}{C}(\nabla C \cdot \nabla C) \tag{18}$$

The second, third, and forth terms in Eqs. (14) can be expanded for the present case as

$$\dot{e}_2' = -\frac{k}{T'^2}\left[\left(\frac{\partial T'}{\partial r'}\right)^2 + \left(\frac{1}{r'}\frac{\partial T'}{\partial\theta}\right)^2\right] \tag{19}$$

$$\dot{e}_3' = -\frac{\rho^g \mathcal{D}^g}{C}\left[\left(\frac{\partial C}{\partial r'}\right)^2 + \left(\frac{1}{r'}\frac{\partial C}{\partial\theta}\right)^2\right] \tag{20}$$

$$\dot{e}_4' = -\frac{\bar{s}_v}{T'}\left[\frac{\partial C}{\partial r'}\frac{\partial T'}{\partial r'} + \frac{1}{r'^2}\frac{\partial C}{\partial\theta}\frac{\partial T'}{\partial\theta}\right] \tag{21}$$

Considering the liquid vapor to be an ideal gas, its partial molal entropy $\bar{s}_v$, appearing in Eq. (21) is expressed as

$$\bar{s}_v = R\ln\left(\frac{P_v'}{P_r'}\right) + Cp_v\ln\left(\frac{T'}{T_r'}\right) + \bar{s}_{vr} \tag{22}$$

where $\bar{s}_{vr}$ is the partial molal entropy of the vapor at a reference pressure and temperature P_r' and T_r', respectively.

The total entropy generation rate $\dot{E}'$ at any instant in the process of droplet evaporation is found out by integrating the local entropy generation rate per unit volume over the spatial domain of transport processes in both the carrier and droplet phases as

$$\dot{E}' = \dot{E}^{g\prime} + \dot{E}^{l\prime} \tag{23}$$

where the entropy generation rate in the carrier phase is

$$\dot{E}^{g\prime} = \int_1^\infty\int_0^\pi\int_0^{2\pi}(\dot{e}_1^{g\prime} + \dot{e}_2^{g\prime} + \dot{e}_3^{g\prime} + \dot{e}_4^{g\prime})\, r'^2\sin\theta\, dr'\, d\theta\, d\phi = \dot{E}_1^{g\prime} + \dot{E}_2^{g\prime} + \dot{E}_3^{g\prime} + \dot{E}_4^{g\prime} \tag{24}$$

and the entropy generation rate in the liquid phase is

$$\dot{E}^{l\prime} = \int_0^1\int_0^\pi\int_0^{2\pi}(\dot{e}_1^{l\prime} + \dot{e}_2^{l\prime})r'^2\sin\theta\, dr'\, d\theta\, d\phi = \dot{E}_1^{l\prime} + \dot{E}_2^{l\prime} \tag{25}$$

In the absence of any mass transfer in the liquid phase, the third and fourth terms ($\dot{e}_3'$ and $\dot{e}_4'$) of the generalized Eqs. (14) do not appear in Eqs. (25).

The nondimensional entropy generation rate is defined as

$$\dot{E} = \frac{\dot{E}'}{\rho_{ai} R_\infty U_\infty a_i'^2} \tag{26}$$

To evaluate the nondimensional entropy generation rate, the variables in Eqs. (24) and (25) are replaced by their nondimensional counterparts. With the help of Eqs. (15), (19–21), and (26), the nondimensional forms of $\dot{e}_1'$, $\dot{e}_{22}'$, etc., in Eqs. (24) and (25) can finally be expressed as

$$\dot{e}_1^g = \frac{2a}{Re_i}Ec\frac{\gamma}{\gamma-1}\frac{\mu^g}{\mu_i^g}\frac{\rho_i}{\rho_{ai}}\frac{1}{T^g}\left\{2\left(\frac{\partial V_r^g}{\partial r}\right)^2 + 2\left(\frac{1}{r}\frac{\partial V_\theta^g}{\partial\theta} + \frac{V_\theta^g}{r}\right)^2 + 2\left(\frac{V_r^g}{r} + \frac{V_\theta^g\cot\theta}{r}\right)^2 + \left[r\frac{\partial}{\partial r}\left(\frac{V_\theta^g}{r}\right) + \frac{1}{r}\frac{\partial V_r^g}{\partial\theta}\right]^2\right\} \tag{27}$$

$$\dot{e}_1^l = \frac{2a}{Re}Ec\frac{\gamma}{\gamma-1}\frac{\mu^l}{\mu_i^g}\frac{\rho^g}{\rho_{ai}}\frac{1}{T^l}\left\{2\left(\frac{\partial V_r^l}{\partial r}\right)^2 + 2\left(\frac{1}{r}\frac{\partial V_\theta^l}{\partial\theta} + \frac{V_\theta^l}{r}\right)^2 + 2\left(\frac{V_r^l}{r} + \frac{V_\theta^l\cot\theta}{r}\right)^2 + \left[r\frac{\partial}{\partial r}\left(\frac{V_\theta^l}{r}\right) + \frac{1}{r}\frac{\partial V_r^l}{\partial\theta}\right]^2\right\} \tag{28}$$

$$\dot{e}_2^g = \frac{2a}{Pe_i^g}\frac{k^g}{k_i^g}\frac{Cp^g}{Cp_\infty}\frac{\rho_i^g}{\rho_{ai}}\frac{\gamma}{\gamma-1}\frac{1}{T^{g2}}\left[\left(\frac{\partial T^g}{\partial r}\right)^2 + \left(\frac{1}{r}\frac{\partial T^g}{\partial\theta}\right)^2\right] \tag{29}$$

$$\dot{e}_2^l = \frac{2a}{Pe_i^g}\frac{k^l}{k_i^g}\frac{Cp^g}{Cp_\infty}\frac{\rho_i^g}{\rho_{ai}}\frac{\gamma}{\gamma-1}\frac{1}{T^{l2}}\left[\left(\frac{\partial T^l}{\partial r}\right)^2 + \left(\frac{1}{r}\frac{\partial T^l}{\partial\theta}\right)^2\right] \tag{30}$$

$$\dot{e}_3^g = \frac{2a}{Pe_i^g Le_i^g}\frac{W_\infty}{W_v}\frac{\rho^g}{\rho_{ai}}\frac{\mathcal{D}^g}{\mathcal{D}_i^g}\frac{1}{C}\left[\left(\frac{\partial C}{\partial r}\right)^2 + \left(\frac{1}{r}\frac{\partial C}{\partial\theta}\right)^2\right] \tag{31}$$

$$\dot{e}_4^g = \frac{2a}{Pe_i^g Le_i^g}\frac{\rho^g}{\rho_{ai}}\frac{\mathcal{D}^g}{\mathcal{D}_i^g}\frac{\bar{s}_v}{R_\infty W_v}\frac{1}{T^g}\left[\frac{\partial C}{\partial r}\frac{\partial T^g}{\partial r} + \frac{1}{r^2}\frac{\partial C}{\partial\theta}\frac{\partial T^g}{\partial\theta}\right] \tag{32}$$

Method of Solution

Equations (1–5) were solved simultaneously at each and every time step with the aid of the finite difference method. For the solutions of equations in the carrier phase [Eqs. (1a), (1b), and (3–5)] the radial coordinate r was transformed to z as $r = e^z$ for the use of a constant step size for z to obtain a denser mesh near the surface, as suggested earlier by several workers such as Woo and Hamielec[19] and Abramzon and Elata.[20] However, no such transformation was made for the solution of equations in the droplet phase. Quasisteady solutions of Eqs. (1–3) and (5) were carried out by the method of iteration with a successive over relaxation (SOR) scheme, as reported earlier by Woo and Hamielec.[19] A discretization scheme and the finite difference forms of the momentum equations [Eqs. (1a) and (1b)] can be found in Hamielec et al.[14]; those of energy and species continuity equations [Eqs. (3) and (5)] are found in Woo and Hamielec.[19] The momentum equations were first solved by the Galerkin method in order to generate the initial guess values for the iterative scheme. The relaxation parameters for the solutions of mo-

mentum equations were taken to be 0.4 for $Re < 10$, 0.2 for $10 \leq Re < 20$, 0.1 for $20 \leq Re < 50$, and 0.05 for $50 \leq Re < 100$, which are in accordance with those of LeClair et al.[21] The relaxation parameters for the solution of energy and species continuity equations were kept at 0.6 for $Pe^g < 10$, 0.5 for $10 \leq Pe^g < 40$, and 0.4 for $Pe^g > 40$. Numerical experiments for testing of grid sizes in the case of evaporating drop were made as follows.

In the carrier phase, for $Re = 10$, mesh sizes ($\Delta z \times \Delta\theta$) of 0.1 × 9°, 0.075 × 6°, and 0.05 × 4° with $Z_\infty = 3$, 4, and 4, respectively, were used. It was observed that a mesh size finer than 0.075 × 6° produced insignificant changes in the value of Nu and C_D. However, for $Re_i > 50$, grid size testing was not carried out because of the large computation time on a Domain 3000 Apollo system and a mesh size of 0.05 × 6° was taken as suggested by Sayegh and Gauvin[22] with $Z_\infty = 2.5$. In the droplet phase, a mesh ($\Delta r \times \Delta\theta$) of 0.05 × 6° was used for all of the conditions. The finite difference forms of Eqs. (1–3) and (5) were iterated at each and every time step until the difference in the successive values of Nu was <0.005%. Equation (4) was solved by an alternate direction implicit (ADI) scheme with forward marching along the time direction. The time step Δt was kept at 0.0001 at the beginning of the solution and was slowly changed to 0.0005 when the droplet mass had attained a value of 0.95. This time step was kept almost constant until the droplet mass had attained a value near about 0.3. Then the time step was slowly decreased to 0.0001 or less, as the droplet mass was gradually depleted. The instantaneous drop radius was determined from Eq. (11a) by the explicit method with the initial condition as $a = 1$ at $t = 0$. In the computational scheme, the droplet lifetime refers to the instant when approximately 95% of the mass had evaporated, which corresponds to the value of $a \cong 0.36$. The computation was not carried out beyond this time. The entropy generation rate at each instant was calculated by integrating Eqs. (24) and (25). The triple integrals in Eqs. (24) and (25) are reduced to double integrals because of the symmetry in ϕ. Then, the double integrals were integrated by Simpson's ⅓ rule after evaluating the local entropy generation rate ($\dot{e}_1^g$, $\dot{e}_2^g$, etc.) in Eqs. (27–32). The values of $\dot{e}_{11}^g$, $\dot{e}_2^g$, etc., were calculated by the finite difference scheme after the evaluation of the velocity, temperature, and concentration fields at each and every instant.

Air was taken as the freestream ambience, and the studies were made with liquid drops of water benzene, ethanol, n-Hexane, and n-Decane. The initial drop temperature for all of the cases was taken as 293K, and the reference state for $\bar{S}_{vr}$ values shown in Eq. (22) were taken as the saturated vapor state of the liquids under normal boiling conditions (101.35 kPa). Carrier phase was considered to be a mixture of ideal gases (air and liquid vapor) and its thermophysical properties were assumed to be spatially constant. The property values were evaluated at film conditions (at a reference temperature and vapor mass fraction that are the arithmetic averages of those values at drop surface and at freestream, respectively) with the help of Reid et al.[23]

Results and Discussions

Transport Coefficient

An average Nusselt number Nu has been evaluated in the present case for the purpose of their comparisons with the relevant values available in the literature. A comparison of the present numerical data of the average Nusselt number has been made (Fig. 2) with the widely referred empirical equations due to Ranz and Marshall[24] with a B number correction factor, already established in several earlier works due to Agoston et al.[25] and Yuen and Chen,[26] which is given by

$$Nu(1 + B) = 2 + 0.6\, Re_M^{0.5} Pr^{0.33} \tag{33}$$

A fair agreement of predicted Nu in transient zone with those from steady-state empirical equations [Eq. (33)] requires a modified value of heat of vaporization for the liquid, due to the heat flux in the drop, to be used in those equations [Eq. (33)]. Modified Marshall's[1] correlation [Eq. (33)] fits best with the predicted values in the entire range and is shown in Fig. 2. All properties defining Re_M and Pr in Eq. (33) are referred to those at film conditions except for density in the Reynolds number Re_M, which is the freestream density ρ_∞. Therefore, for the purpose of comparison, the Reynolds number Re of

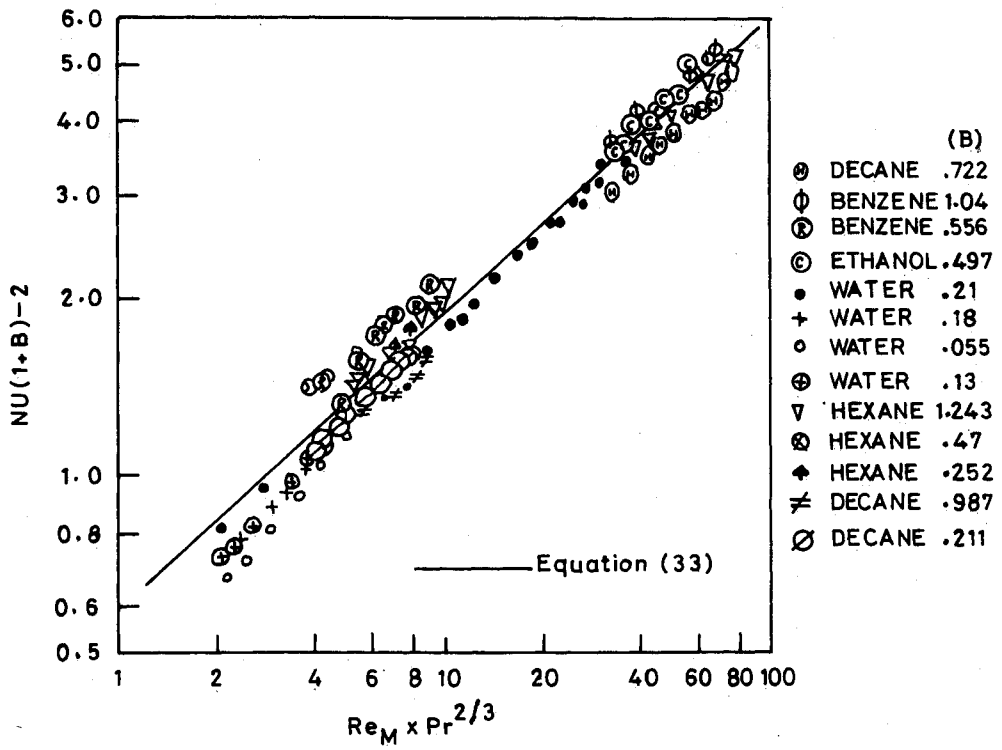

Fig. 2 Comparisons of numerical Nu with empirical correlation from literature.

Table 1 Comparisons of total entropy generation rate due to different modes of transport processes in gas and liquid phases for an evaporating water drop ($P'_\infty/P'_a = 10$, $T_\infty = 2.9$, $Ec = 10^{-3}$, $Re_i = 10$)

t	Re	$\dot{E}_1^g$	$\dot{E}_1^l$	$\dot{E}_2^g$	$\dot{E}_2^l$	$\dot{E}_3^g$	$\dot{E}_4^g$
0.018	9.4	0.01	4.0×10^{-4}	18.7	0.91	0.09	0.42
0.128	8.8	0.01	5.5×10^{-4}	16.7	0.80	0.20	0.99
0.687	7.0	0.01	7.7×10^{-4}	11.8	0.16	2.57	9.10
1.528	6.1	0.01	7.8×10^{-4}	12.0	5.1×10^{-3}	6.15	17.5
2.167	5.7	0.012	7.8×10^{-4}	13.7	5.5×10^{-4}	6.68	20.2
2.970	5.2	0.015	7.9×10^{-4}	15.7	5.8×10^{-4}	7.22	22.5
3.680	5.7	0.016	7.9×10^{-4}	17.2	6.6×10^{-4}	7.83	24.4
4.643	3.9	0.020	8.0×10^{-4}	19.8	7.2×10^{-4}	8.41	28.1
5.213	3.4	0.033	8.1×10^{-4}	21.5	7.8×10^{-4}	9.16	31.3
5.683	2.9	0.038	8.2×10^{-4}	24.1	9.0×10^{-4}	10.1	35.1

the present work was scaled to Re_M to read the corresponding numerical data of Nu.

Thermodynamic Irreversibility

Thermodynamic irreversibilities in the process of droplet evaporation are characterized by the instantaneous rate of entropy production in the transport processes, as calculated from Eq. (23). It is observed that the entropy generation rate due to viscous dissipation is very small because of very low Eckert numbers encountered in these cases. It is for the same reason that the dissipation function in the energy equation is neglected. Though this term is included in the general formulation for entropy generation rate [Eq. (27)], the computed values show that the term is always 2–3 orders of magnitude less than the other terms (Table 1). Irreversibilities in the droplet phase, as determined from Eqs. (25), are found to be quite insignificant compared to those in the carrier phase (Table 1). The most significant contribution in the total entropy generation rate are due to the conduction of heat and its coupled effect with mass transfer in the carrier phase. The entropy generation rate $\dot{E}'$ always decreases with time along with the decrease in droplet mass. In the present theoretical formulation, the nondimensional entropy generation rate per unit surface area ($\dot{E}/a^2$) is expressed as a function of pertinent variables, namely, Reynolds number Re, Prandtl number Pr, ratio of molecular weights of liquid to free stream gas Wv/W_∞, and transfer number B. The value of $\dot{E}/a^2$ increases continuously until the end of the evaporation process (Figs. 3 and 4). This implies that the droplet surface area decreases at a faster rate than that of the decrease in the entropy generation rate. An explicit form of the functional relationship of $\dot{E}/a^2$ with the pertinent parameters, as described earlier, has been developed from the present numerical experiments (with 250 data points) by least square regression analysis as

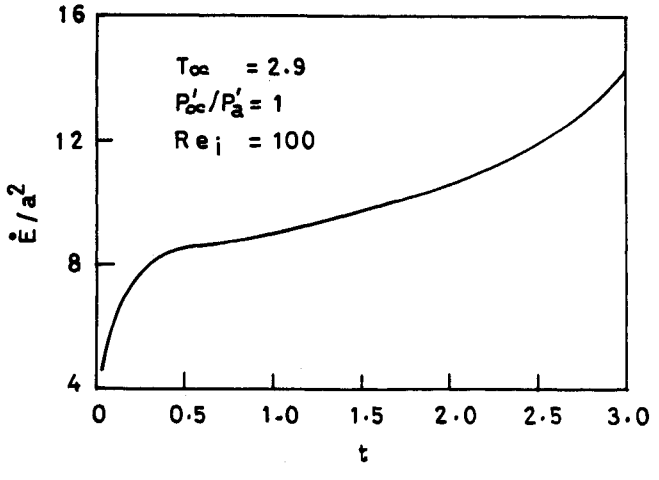

Fig. 3 Temporal histories of $\dot{E}$ for a water droplet.

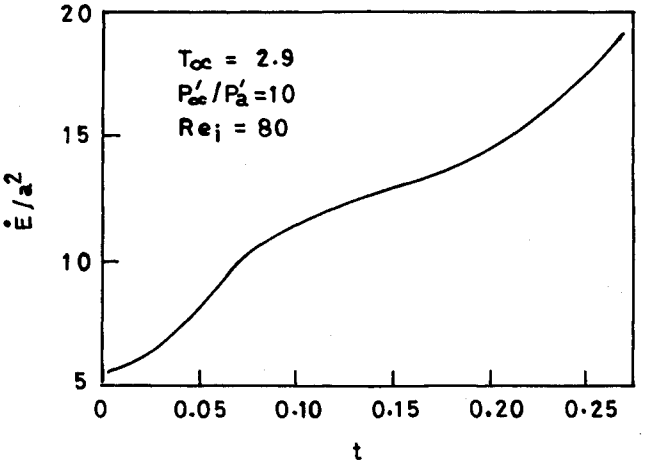

Fig. 4 Temporal histories of $\dot{E}$ for a Hexane droplet.

$$\frac{\dot{E}}{a^2} = 714.49 \left(Re\, Pr^{0.66}\right)^{-0.724} \left(\frac{W_\infty}{Wv}\right)^{1.024} B^{1.288} \quad (34)$$

Equation (34) shows a maximum relative error [the difference between the numerically generated data points and those determined from the best fit curve (Eq. 34)] of 15%. This maximum error is exhibited by <4% of the total data points, whereas the root mean square value of the relative errors over the entire range of numerical experiment is 4.18%. The numerically predicted values along with the best fit curve [Eq. (34)] are shown in Fig. 5. An increase in Reynolds number Re accompanied by an increase in either the freestream velocity U_∞ or the initial drop radius a'_i, in fact, increases both the heat transfer and entropy generation rates. However, a decrease in nondimensional entropy generation rate $\dot{E}$ with the increase in Re as shown by Eq. (34) is due to the typical normalization scheme of entropy generation rate $\dot{E}'$ by Eq. (26), where U_∞ has been taken as the reference variable in the denominator. To avoid this apparent confusion, one can define a separate nondimensional scheme of $\dot{E}'$ as distinct from Eq. (26) as

$$\dot{E} = \frac{E'}{(\rho_{ai}\, R_\infty\, \alpha_i^g a_i')} \quad (35)$$

With the help of Eq. (35), Eq. (34) can be transformed to another form as

$$\frac{\dot{E}}{a} = 357.25\, Re^{0.276} Pr^{0.517} \frac{\alpha^{-g}}{\alpha_i^g} \left(\frac{W_\infty}{Wv}\right)^{1.024} B^{1.288} \quad (36)$$

Where E, the nondimensional version of entropy generation rate, is defined by Eq. (35) instead of Eq. (26). Any one of

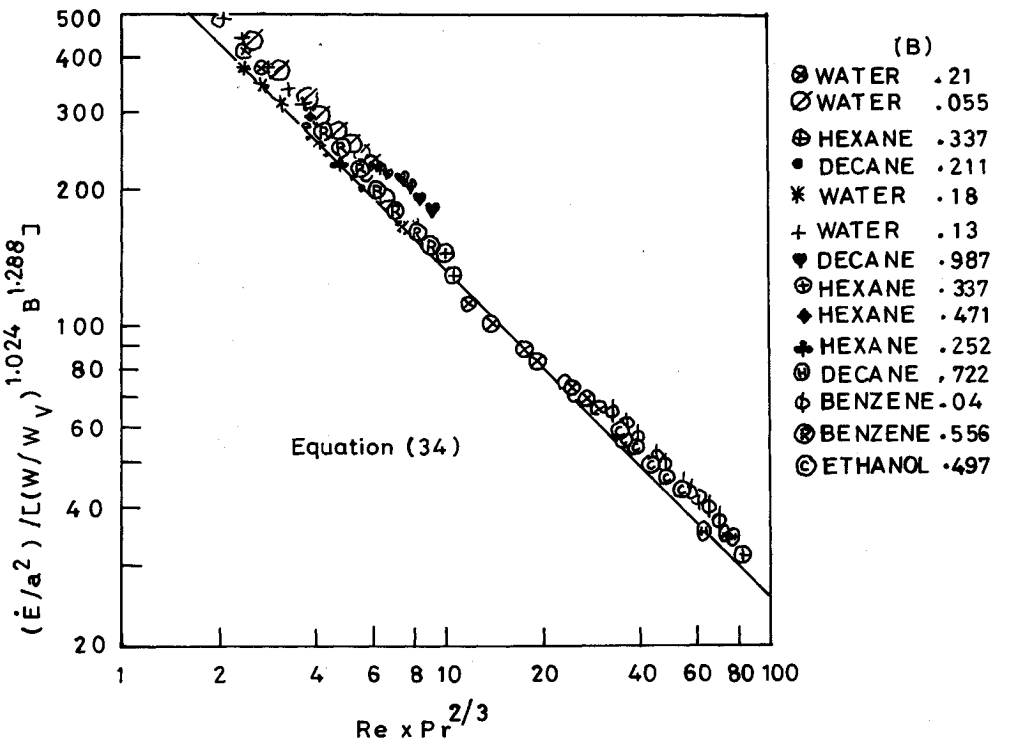

Fig. 5 Law of entropy generation rate in steady-state evaporation process.

Eqs. (34) and (36) describe the entropy generation rate in the process of evaporation of a single drop in terms of the pertinent controlling parameters and will serve as the fundamental input to the second law analysis of spray evaporation—an important thermodynamic aspect of spray modeling.

Conclusions

Thermodynamic irreversibilities in the process of droplet evaporation are mainly due to the conduction of heat and coupled effect of heat and mass convection in the carrier phase. The rate of entropy production during the droplet evaporation decreases continuously at a rate lower than the decreasing rate of droplet surface area. The nondimensional entropy generation rate [defined by Eq. (34)] per unit droplet surface area bears an inverse power relationship with Re and Pr and a direct relationship with B and W_∞/W_V. The explicit form of the generalized functional relation relating the entropy generation rate with the pertinent variables has been developed as a requirement of the fundamental information to the energy analysis of spray evaporation—the important thermodynamic aspect of spray modeling.

References

[1]Marshall, W. R., Jr., *Atomization and Spray Drying*, Chemical Engineering Monograph Series, No. 2, Vol. 50, American Inst. of Chemical Engineers, New York, 1954.

[2]Clift, R., Grace, J. R., and Weber, M. E., *Bubbles, Drops and Particles*, Academic Press, New York, 1978.

[3]Law, C. K., "Recent Advances in Droplet Vaporization," *Progress Energy Combustion Science*, Vol. 8, 1982, pp. 171–201.

[4]Faeth, G. M., "Evaporation and Combustion of Sprays," *Progress Energy Combustion Science*, Vol. 9, 1983, pp. 1–76.

[5]Sirignano, W. A., Fuel Droplet Vaporization and Spray Combustion Theory," *Progress Energy Combustion Science*, Vol. 9, 1983, pp. 291–322.

[6]Sirignano, W. A., "An Integrated Approach to Spray Combustion Model Development," *Combustion Science and Technology*, Vol. 58, 1988, pp. 231–251.

[7]Prakash, S., and Sirignano, W. A., "Theory of Convective Droplet Vaporization with Unsteady Heat Transfer in Circulating Liquid Phase," *International Journal of Heat and Mass Transfer*, Vol. 23, 1980, pp. 253–268.

[8]Lara-Urbanega, P., and Sirignano, W. A., "Theory of Transient Multicomponent Droplet Vaporization in a Convective Field," *Proceedings of the Eighteenth Symposium (International) on Combustion*, Combustion Inst., 1981, pp. 1365–1374.

[9]Renksizbulut, M., and Yuen, M. C., "Numerical Study of Droplet Evaporation in a High Temperature Air Stream," *ASME Journal of Heat Transfer*, Vol. 105, May 1983, pp. 389–397.

[10]Dwyer, H. A., and Sanders, B. R., "Comparative Study of Droplet Heating and Vaporization at High Reynolds and Peclet Numbers," *Progress in Astronautics and Aeronautics*, Vol. 95, AIAA, New York, 1984, pp. 464–483.

[11]Oliver, D., and Chung, J., "Conjugate Unsteady Heat Transfer from a Spherical Droplet at Low Reynolds Number," *International Journal of Heat and Mass Transfer*, Vol. 29, 1986, pp. 879–887.

[12]Renksizbulut, M., and Haywood, R. J., "Transient Droplet Evaporation with Variable Properties and Internal Circulation at Intermediate Reynolds Number," *International Journal of Multiphase Flow*, Vol. 14, No. 2, 1988, pp. 189–202.

[13]Sundarrajan, T., and Ayyaswamy, P. S., "Hydrodynamics and Heat Transfer Associated with Condensation on a Moving Drop: Solution for Intermediate Reynolds Number," *Journal of Fluid Mechanics*, Vol. 149, 1984, pp. 33–58.

[14]Hamielec, A. E., Hoffman, T. W., and Ross, L. L., "Numerical Solution of Navier-Stokes Equation for Flow Past Spheres, Part I, Viscous Flow Around Spheres With and Without Mass Efflux, *AIChE Journal*, Vol. 3, 1967, p. 212–217.

[15]Harpole, G. M., "Droplet Evaporation in High Temperature Environment," *ASME Journal of Heat Transfer*, Vol. 103, 1981, pp. 86–91.

[16]Krikwood, J. G., and Crawford, B., Jr., "The Macroscopic Equation of Transport," *Journal of Physical Chemistry*, Vol. 56, 1952, pp. 1048–1051.

[17]Bird, R. B., Stewart, W. E., and Lightfoot, E. N., *Transport Phenomena*, Wiley, New York, 1960, pp. 91.

[18]Denbigh, D., The Principle of Chemical Equilibrium, 4th ed., Cambridge University Press, Cambridge, MA, 1981.

[19]Woo, S. E., and Hamielec, A. E., "A Numerical Method of Determining the Rate of Evaporation of Small Water Drops Falling at Terminal Velocity in Air," *Journal of the Atmospheric Sciences*, Vol. 28, 1971, pp. 1448–1454.

[20]Abramzon, B., and Elata, C., "Unsteady Heat Transfer from a Single Sphere in Stokes Flow," *International Journal of Heat and Mass Transfer*, Vol. 27, No. 5, 1984, pp. 687–695.

[21]LeClair, B. P., Hamielec, A. E., and Pruppacher, H. R., "Nu-

merical Study of the Drag on a Sphere at Low and Intermediate Reynolds Numbers," *Journal of Atmospheric Sciences*, Vol. 27, 1970, pp. 308–315.

[22]Sayegh, N. N., and Gauvin, W. H., "Numerical Analysis of Variable Property Heat Transfer to a Single Sphere in High Temperature Surroundings," *AIChE Journal*, Vol. 25, 1979, pp. 522–527.

[23]Reid, R. C., Prausnitz, J. M., and Sherwood, T. K., *The Properties of Gases and Liquids*, 3rd ed., McGraw-Hill, New York, 1977.

[24]Ranz, W. E., and Marshall, W. R., Jr., *Evaporation from Drops, Part II, Chemical Engineering Progress*, Vol. 48, 1952, pp. 173–180.

[25]Agoston, G. A., Wise, H., and Rosser, W. A., "Dynamic Factors Affecting the Combustion of Liquid Spheres, *Proceedings of the Sixth Symposium (International) on Combustion*, 1957, pp. 108–113.

[26]Yuen, M. C., and Chen, L. W., "Heat Transfer Measurements of Evaporating Liquid Droplets, *International Journal of Heat and Mass Transfer*, Vol. 21, 1978, pp. 537–542.